Research Paper

Journal of Engineering and Technological Sciences

Solvent-free Synthesis of Transition Metals Nanoparticles Decorated Foamy Flakes-like Nitrogen-doped Carbon as Bifunctional-catalyst for High-performance Rechargeable Zn-air Batteries

Pilar Bela Persada[1], Davin Adinata Tan[1], Rachendra Akmalia[1], Yuyun Irmawati[2, 3] & Afriyanti Sumboja[1,4,*]

[1]Material Science and Engineering Research Group, Faculty of Mechanical and Aerospace Engineering, Institut Teknologi Bandung, Jalan Ganesa 10, Bandung 40132, Indonesia
[2]Doctoral Program of Nanosciences and Nanotechnology, Graduate School, Institut Teknologi Bandung, Jalan Ganesa 10, Bandung 40132, Indonesia
[3]Research Center for Advanced Materials, National Research and Innovation Agency (BRIN), Kawasan Puspiptek Gedung 440, Tangerang Selatan 15314, Indonesia
[4]Collaboration Research Center for Advanced Energy Materials, National Research and Innovation Agency – Institut Teknologi Bandung, Jalan Ganesa 10, Bandung 40132, Indonesia

*Corresponding author: sumboja@itb.ac.id

Abstract

Transition metal-nitrogen-carbon (M/NC) demonstrates a promising effective electrocatalyst for enhancing oxygen evolution/reduction reactions (OER/ORR). However, synthesizing these catalysts is often complex, time-consuming, and involves hazardous solvents while producing a low yield. This work introduces a versatile, eco-friendly, and straightforward solvent-free method to produce M/NC (M = Co, Ni, and Fe) catalysts in ~3 h using a glucose, urea, and metal nitrate hydrate mixture. The high-yield M/NC catalysts exhibit a porous architecture and uniform distribution of metal nanoparticles within a foaming flakes-like nitrogen-doped carbon matrix. The metal nanoparticles are wrapped with protective nitrogen-doped carbon layers, producing stable active sites. Possessing these unique properties, the obtained M/NC catalysts show high-performance and stable bifunctional OER/ORR. As the best result, Co/NC presents an OER/ORR potential difference (ΔE) of 0.78 V and retains 96% and 89% of its OER and ORR performance after a 10 h stability test. In practical application, the Co/NC-based Zn-air battery depicts a high power density of 184 mW cm^{-2} and good rechargeability of up to 120 h, outperforming the battery with noble metal-based catalysts. This work sheds light on the versatile, eco-friendly, and scalable synthesis of M/NC catalysts while presenting a strategy to accelerate the generation of inexpensive and highly effective bifunctional OER/ORR catalysts.

Keywords: *electrocatalysis; non-noble metal catalysts; oxygen evolution reaction; oxygen reduction reaction; zinc-air battery.*

Introduction

Rechargeable Zn-air batteries are currently garnering attention owing to their remarkable theoretical energy densities (1086 Wh kg^{-1}) as well as using non-toxic and non-flammable aqueous electrolytes [1, 2]. They are also known for their cost-effectiveness in production, as they utilize abundant and inexpensive Zn metal [3]. However, rechargeable Zn-air batteries are still facing some challenges involving the utilization of noble-metal catalysts, including iridium (Ir), ruthenium (Ru), and platinum (Pt), which are employed to enhance oxygen evolution or reduction reactions (OER or ORR) that is crucial for the rechargeability process [1]. These noble-metal catalysts have limitations: facilitating only the OER or ORR (i.e., monofunctional catalyst), inferior stability, high cost, and limited resources [4, 5]. Hence, there is a compelling need to fabricate bifunctional OER/ORR catalysts utilizing plentiful non-noble metal resources, which may effectively support extensive utilization in large-scale applications [6, 7].

Studies have revealed the important role of metal-nitrogen-carbon (M/NC with M = Co, Ni, and Fe) materials as one of the most promising candidates for bifunctional OER/ORR catalysts [8-10]. Owing to the unique interaction between the anchored transition metal and the nitrogen-doped carbon matrix, both physical and chemical properties of the catalysts

ISSN: 2337-5779
J. Eng. Technol. Sci. Vol. 56, No. 5, 2024, 666-678
DOI: 10.5614/j.eng.technol.sci.2024.56.5.10

DOI: 10.5614/j.eng.technol.sci.2024.56.5.10

can be finely tuned, resulting in outstanding activity, fast electron transfer ability, high atomic utilization, superior electronic conductivity, and excellent durability of the catalysts [11-13]. Incorporating Co nanoparticles on nitrogen-doped carbon nanotubes, Liu et al. obtained a Co/NC-based bifunctional catalyst with an overpotential of 500 mV for OER and an onset potential of 0.89 V for ORR [14]. Ma et al. synthesized Fe-N_x active sites that were evenly distributed over a porous nitrogen-doped carbon material with a graphitic structure and exhibited OER overpotential and ORR onset potential of 390 mV and 0.997 V, respectively [15]. In another study, Liu et al. prepared Ni nanoparticles anchored on carbon nanofiber, displaying OER overpotential and ORR onset potential of 293 mV and 0.93 V [16].

Despite those significant advancements in M/NC-based catalysts, their synthesis often involves typical wet chemical routes that include numerous stages and cumbersome processes, resulting in a lengthy synthesis time. For example, Choi et al. employed wet chemical procedures involving about two days of the reaction process with two annealing steps to obtain nitrogen-doped carbon nanotubes with Co nanoparticles encased within them [17]. Jieting Ding and coworkers produced Fe/NC-based catalyst via a multi-step process: dissolving the precursors and freeze-drying step (12 h), ball-milling the dried sample (6 h), pyrolyzing at 900 ℃(2 h), and finally drying for 12 h in a vacuum oven [18]. Besides that, some wet synthetic routes also include the use of hazardous and organic solvents [19], such as perchloric acid [20], sulfuric acid [21], phosphoric acid [22], N, N-dimethylformamide [23], and methanol [24]. In addition, due to its low yield, it is challenging to adopt the wet chemical approach to pursue economic benefits practically [25]. Therefore, it is imperative to establish a simple, eco-friendly, and practical method for developing bifunctional electrocatalysts.

As an alternative to wet chemical methods, solvent-free synthesis methods are regarded as the efficient synthesis procedure. These methods minimize the production of waste and pollution risks during chemical processes, resulting in enhanced environmental sustainability compared to wet chemical methods [25]. It also offers other benefits, such as low setup and energy costs, economic viability, easy operation, time efficiency, and high-yield products [26]. Herein, we demonstrate the versatility of this solvent-free method to synthesize transition metal nanoparticles decorated with foamy flakes-like nitrogen-doped carbon matrix. Glucose, urea, and metal nitrate hydrate were dry-mixed and subjected to a fast melting-drying process to obtain the foam-like structure. The obtained M/NC catalysts exhibited a porous-rich architecture with a homogeneous distribution of metal nanoparticles across the foamy flakes-like carbon matrix layers, resulting in highly accessible catalytic sites. Benefiting these characteristics, the obtained M/NC catalyst performs high OER and ORR activities, leading to favorable performance of rechargeable Zn-air battery. This study establishes an environmentally friendly and economically efficient method for producing affordable and highly efficient bifunctional electrocatalysts, supporting the development of rechargeable Zn-air battery technologies.

Experimental Procedure

Preparation of Co/NC

In a typical procedure, 2 g of glucose (≥99.5%, Merck), 0.5 g of urea (≥99%, Merck), and 2 g of cobalt nitrate hydrate (98%, Merck) were dry mixed to form a homogeneous mixture by continuous stirring for 30 min. Afterward, the resultant mixture was heated until the melting state using an oil bath at 120 ℃ (~5 min). The obtained homogenized fluid mixture product was then quickly transferred to a preheated oven at 180 ℃for 20 min, forming the foam-like structure. In the next step, the obtained solid product was pyrolyzed in a nitrogen environment at 800 ℃with holding duration of 2 h. The resulting material was ground into a fine black powder upon reaching ambient temperature, yielding Co/NC catalyst. For comparison, a control sample of nitrogen-doped carbon (NC) was prepared without adding cobalt nitrate hydrate. Furthermore, to demonstrate the versatility of the proposed method, a similar procedure was also used to synthesize Ni/NC and Fe/NC, where Ni nitrate hydrate (≥94.5%, Merck) and Fe nitrate hydrate (≥98%, Merck) was employed as the metal precursor.

Materials Characterization

Morphologies and elemental distributions were analyzed using field-emission scanning transmission electron microscopy (SEM, JEOL JIB 4610F) equipped with energy dispersive X-ray spectroscopy (EDS) and transmission electron microscopy (TEM, FEI Tecnai G2 20S). X-ray diffraction (XRD) was determined using Rigaku SmartLab. Raman spectra were determined using Horiba Modular Raman iHR320. X-ray photoelectron spectrometer (XPS) spectra were acquired using Kratos AXIS Supra$^+$. Surface area and pore dimensions were analyzed via N_2 adsorption/desorption isotherms from the Micromeritics TriStar II instrument. Electrochemical measurement and rechargeable Zn-air battery test were conducted following the established protocols outlined in our previous work [27].

Results and Discussion

The synthesis procedure of M/NC-based catalysts (e.g., Co/NC) via solvent-free method can be seen in Figure 1. Instead of dissolving the cobalt nitrate salt, urea, and glucose, we used a simple dry mixing process to achieve a homogeneous mixture of the precursors. Subsequently, the mixture was melted at 120 ℃ for 5 min before being immediately transferred into a preheated oven (180 ℃, 2 min). The metal nitrate hydrate salt rapidly decomposes during preheating, producing volatile substances, including NO_2, N_2, CO_2, and water vapor [28]. These gases induce the expansion of the molten viscous paste of the precursors, leading to the development of a foam-like structure. In contrast, NC sample that was prepared without any metal nitrate exhibits less foam formation, as evidenced by its smaller volume expansion than that of Co/NC. The obtained dried foam-like material was then pyrolyzed at 800 ℃ (2 h) under an N_2 atmosphere and ground into a fine catalyst powder. Unlike wet chemical approaches, which require around two days to synthesize the catalysts [17, 29], this solvent-free process is far more time-efficient, taking ~3 h, which already includes mixing, heating, and pyrolysis processes. This method could also produce an approximate yield of 20%. Moreover, as the synthesis process is solvent-free, it produces minimal waste and pollutants, rendering it environmentally advantageous.

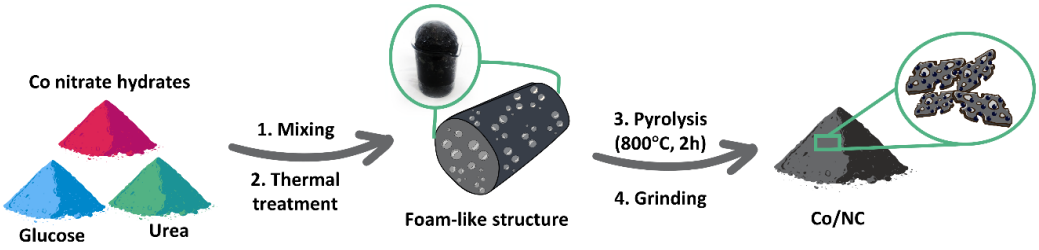

Figure 1 The schematic synthesis procedure of Co/NC via solvent-free method.

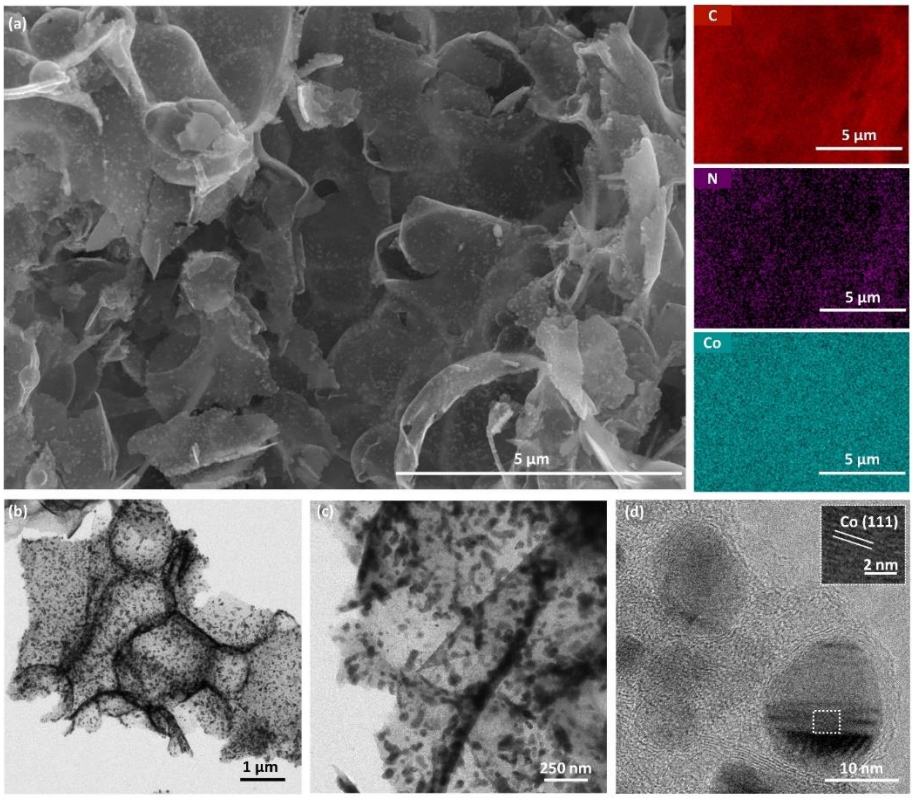

Figure 2 (a) SEM images and EDS mapping of C (red), N (purple), and Co (cyan) elements of as-synthesized Co/NC. (b-c) Low-resolution TEM images that show foam-like structures. (d) The corresponding high-resolution TEM images of Co/NC with inset of Co lattice spacing.

DOI: 10.5614/j.eng.technol.sci.2024.56.5.10

The obtained Co/NC morphological structure was analyzed using SEM images. As depicted in Figure 2(a), SEM images of Co/NC show a foam-like structure consisting of porous flakes with bubble textures. Notably, spherical metal particles in nanosize are also clearly seen homogeneously distributed on the flakes. The elemental composition of Co/NC was then validated by EDS mapping. Co/NC demonstrates an evenly distributed element of C (red), N (purple), and Co (cyan), indicating that the carbon flakes doped with nitrogen are decorated with cobalt nanoparticles. Furthermore, in line with the SEM images, TEM images of Co/NC also show foam-like structures with homogeneously distributed Co nanoparticles (Figure 2(b-c)). In addition, high-resolution TEM (Figure 2(d)) demonstrates metallic Co nanoparticles with a lattice spacing of ~0.203 nm wrapped with nitrogen-doped carbon protective shells with a lattice spacing of ~0.346 nm [30, 31].

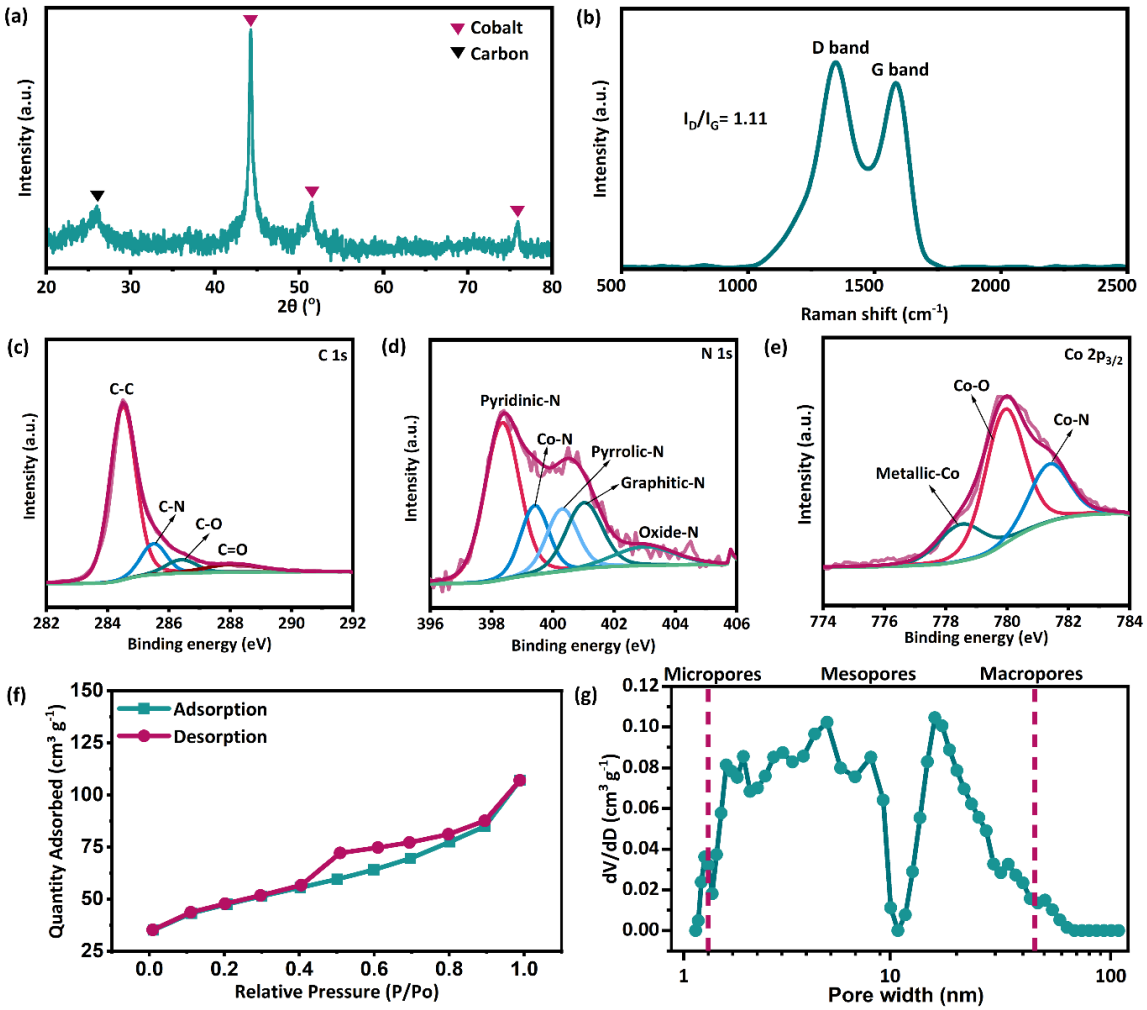

Figure 3 (a) X-ray diffraction pattern, (b) Raman spectra, (c-e) high-resolution C 1s, N 1s, and Co $2p_{3/2}$ XPS spectra of Co/NC. (f) N_2 absorption-desorption isotherm and (g) pore size distribution of Co/NC.

Furthermore, based on the XRD pattern (Figure 3(a)), Co/NC shows sharp peaks at 44.3°, 51.5°, and 75.9° that correspond to the (111), (200), and (220) plane of Co metallic phase (PDF#15-0806) [32]. A small amount of CoO is also found in the samples, as illustrated by a subtle peak at 36.5° belonging to the (111) crystal plane of CoO [33]. A broad peak at around 26° belongs to the (002) plane of carbon [34], indicating successful carbonization of glucose and urea. This carbonization process is also supported by Raman spectra of Co/NC (Figure 3(b)). Peak at 1346.1 cm^{-1} indicates the presence of a defects band, while another peak at 1584.8 cm^{-1} represents the graphitic carbon band [35]. The intensity ratio between I_D and I_G is calculated to determine the degree of defect or graphitization in the carbon matrix [36]. From Figure 3(b), Co/NC exhibits I_D/I_G of 1.11, suggesting a well-balanced degree of graphitization and defect [37]. This may lead to high conductivity and a notable presence of defective sites, contributing to enhanced catalytic activity [38, 39]. The carbon matrix defect is ascribed to the introduction of Co metal and nitrogen doping, demonstrating that Co nanoparticles promote graphitic structure formation during pyrolysis [37, 38].

Chemical states on the surface of Co/NC were then analyzed using XPS. The high resolution of C 1s spectra (Figure 3(c)) shows four deconvolution peaks indexed to C–C (284.5 eV), C–N (285.5 eV), C–O (286.4 eV), and C=O (288.1 eV) [27]. The C–N peak confirms successful nitrogen doping onto the carbon matrix. During the pyrolysis process, glucose and urea, as carbon and nitrogen sources, experience a degradation process, resulting in nitrogen-doped carbon. The high-resolution N 1s spectra (Figure 3(d)) also reconfirm the nitrogen doping. Three N-C bonds, including 41.84% of pyridinic-N (398.4 eV), 18.81% of graphitic-N (401 eV), and 15.28% of Co–N (399.4 eV), are seen along with 15.16% of pyrrolic-N (400.3 eV) and 8.91% of oxide-N (403 eV) [40]. As reported, graphitic-N can enhance electrical conductivity, facilitating fast electron transfer [41, 42]. Graphitic-N and pyridinic-N also function as the OER active sites [43]. In addition, the high relative content of pyridinic-N promotes more oxygen adsorption, thus decreasing the ORR overpotential [43]. For high-resolution Co $2p_{3/2}$ spectra (Figure 3(e)), the metallic-Co peak (778.5 eV) confirms the existence of Co metallic phase, in line with the XRD result. Co–O peaks (779.9 eV) may suggest surface oxidation of the samples, while the Co–N peak (781.4 eV) represents the bonding between Co and nitrogen atoms [44, 45], as also appears in the N 1s spectra. Overall, the chemical state of Co/NC suggests the presence of active sites from nitrogen-doped carbon and metal-containing sites, collectively boosting both OER and ORR [27].

The distribution of pore size and specific surface area of Co/NC were analyzed using N_2 desorption-adsorption. Co/NC has specific surface area of 158 $m^2\ g^{-1}$ and shows type IV isotherm, as indicated by hysteresis loop in the P/P_0 range of 0.4–1 (Figure 3(f)). This suggests the existence of mesopores within the catalyst [46, 47]. Following its isotherm pattern, Figure 3(g) shows that the pores that exist in the material are dominated by mesopores (2-50 nm) with only a small amount of micropores (< 2 nm). Micropore generates more active sites for reactions to occur, while mesopore acts in enhancing mass transport, thus increasing the catalytic activity of Co/NC catalyst [48, 49]. Combining Co metal embedded in nitrogen-doped carbon matrix and highly porous material may benefit in promising OER and ORR catalytic performance [38, 50].

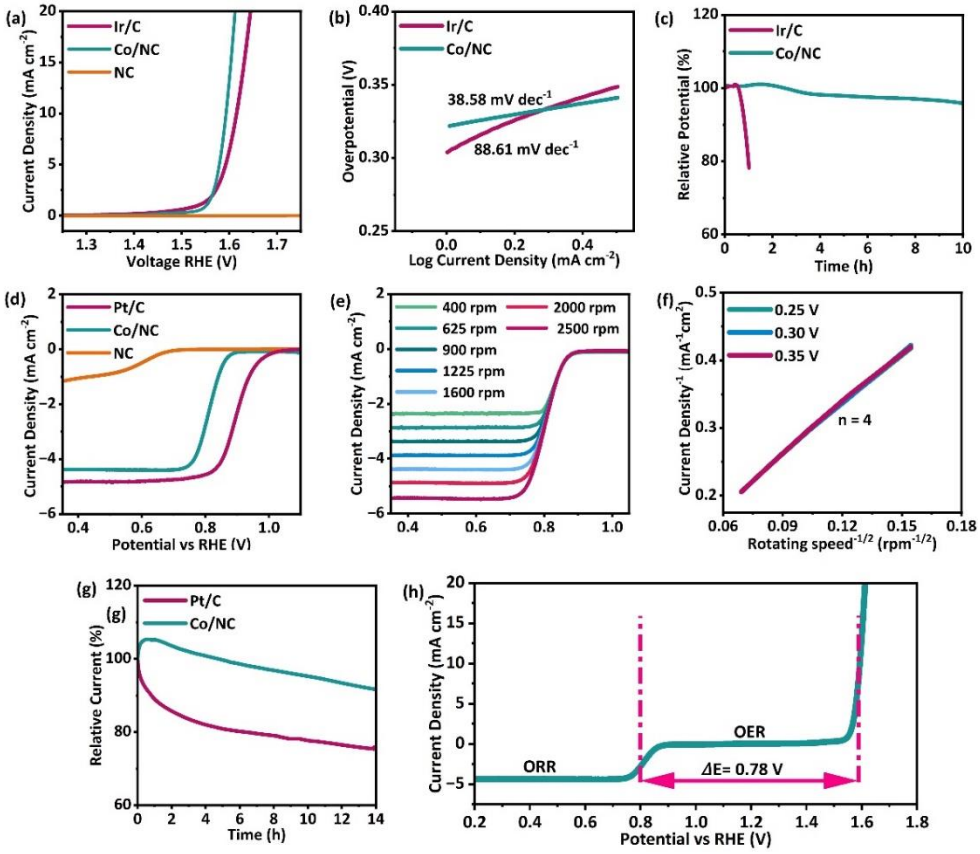

Figure 4 (a) OER polarization curve of Ir/C, Co/NC, and NC, and (b) Tafel slope of Ir/C and Co/NC. (c) OER stability of Ir/C and Co/NC, assessed by chronopotentiometry test at 10 mA cm^{-2}. (d) ORR polarization curve of Co/NC, NC, and Pt/C. (e) ORR LSV curves of Co/NC that are measured at various rotational speeds, and (f) the associated K-L plots. (g) ORR stability of Pt/C and Co/NC, assessed by chronoamperometric test at 0.5 V. (h) The overall polarization curves for bifunctional catalytic activity of Co/NC.

DOI: 10.5614/j.eng.technol.sci.2024.56.5.10

To examine the OER performance, we utilized a rotating disk electrode (RDE) configuration. This setup involved immersing the electrodes in a solution containing 1 M KOH saturated with N_2 to obtain linear sweep voltammograms. The OER overpotential required to generate a current density of 10 mA cm^{-2} on the reversible hydrogen electrode (RHE) potential scale, referred to as η_{10}, was adopted as the main parameter. Ir/C and NC catalysts were also tested in a similar experimental setup for performance comparison. From Figure 4(a), it can be observed that NC can not facilitate the OER which could be due to the absence of metal active sites [51]. Differently, Co/NC exhibits superior OER activity as evidenced by its lower overpotential of 363 mV than Ir/C (388 mV), making it a potential OER catalyst. The high OER activity of Co/NC is also demonstrated by its low Tafel slope of 38.58 mV dec^{-1} (Figure 4(b)), which is approximately half of the Ir/C benchmark (88.61 mV dec^{-1}), suggesting a faster kinetic reaction rate during the OER process [52, 53]. The low overpotential and Tafel slopes of Co/NC can be assigned to the complementary interaction of homogeneous distribution Co nanoparticles anchored in nitrogen-doped carbon foam with porous-rich architecture. This structure enhances performance by providing more accessible active sites and increasing electrical conductivity, thus facilitating fast reactant/electron transfer during reaction [54-56]. The Co/NC also outperforms most of the recently reported Co-based catalysts synthesized via more complicated wet chemical methods, showing overpotential in the 370-450 mV [21, 24, 57, 58]. This result suggests the promising application of a time-efficient solvent-free method to synthesize high-performance OER catalysts.

In order to be practically applicable, catalysts should not only exhibit a high activity but also demonstrate favorable stability [56]. To analyze the OER stability of the catalysts, chronopotentiometry test at 10 mA cm^{-2} was performed. From Figure 4(c), Co/NC can maintain its ~96% performance even after 10 h, surpassing the Ir/C which experiences a rapid decline in performance to around 78% within just 1 h of the chronopotentiometry test. This poor stability of Ir/C is similar to the finding in prior study [59]. The high stability of Co/NC may be attributed to the presence of Co nanoparticles wrapped with nitrogen-doped carbon protective layers, as seen from TEM images. This protective layer prevents direct interaction between the Co nanoparticles and the electrolyte, thus avoiding metal dissolution during catalytic reactions in harsh environments and increasing the catalyst stability [57].

RDE setup was also used to quantify the Co/NC activity towards ORR in 0.1 M KOH. The benchmark of ORR activity was Pt/C catalyst. Limiting current density (J_L), half-wave potential ($E_{1/2}$), and onset potential (E_{onset}) were used as the main parameters to investigate the ORR performance. From Figure 4(d), Co/NC shows a significant increase in the ORR performance compared to NC. Co/NC has J_L, $E_{1/2}$, and E_{onset} of 4.38 mA cm^{-2}, 0.81 V, and 0.9 V, respectively, while the values are 1.6 mA cm^{-2}, 0.6 V, and 0.67 V for the NC. Despite exhibiting somewhat less performance compared to Pt/C (J_L: 4.83 mA cm^{-2}, $E_{1/2}$: 0.89 V, and E_{onset}: 1.02 V), Co/NC shows comparable performance to some reported Co-based catalysts [60-63]. Afterward, we examined the ORR selectivity of Co/NC catalysts using the Koutecky-Levich (K-L) equation in conjunction with linear sweep voltammetry (LSV) measurements at various rotation speeds (Figure 4(e)). Co/NC shows an average electron transfer number of about 4 (Figure 4(f)), indicating a high selectivity of Co/NC to the four-electron ORR process [64]. ORR stability of Co/NC was then evaluated using chronoamperometry test at 0.5 V. Following the 10 h chronoamperometry test (Figure 4(g)), Co/NC can sustain a relative current of about 89%, outperforming Pt/C which declines significantly to about 77%. This result suggests a high ORR stability of the Co/NC catalyst.

For rechargeable Zn-air batteries, both high OER/ORR performances are required during the charging and discharging process. We then calculate the difference between OER potential at 10 mA cm^{-2} and $E_{1/2}$ of ORR, namely $\triangle E$. Co/NC exhibits $\triangle E$ of about 0.78 V (Figure 4(h)), which is competitive compared to other similar catalysts reported before in the difference potential range of 0.76-0.87 V [65-69]. Based on the material characterization provided above, the preceding results toward favorable OER/ORR activity of Co/NC are related to the following key factors: (i) the synergetic effects between nitrogen-doping and homogeneous distribution of Co nanoparticles on carbon matrix lead to a balance between good electrical conductivity and high content defect sites of Co/NC [37, 38]. It facilitates effective charge transfer during reactions and provides numerous active sites [21, 70, 71]. (ii) The foam-like Co/NC with a porous-rich structure ensures a good reactant transfer and provides highly accessible catalytic active sites [72, 73]. (iii) Co nanoparticles encapsulated with nitrogen-doped carbon layers may minimize metal dissolution because of the indirect contact between metal nanoparticles and electrolyte, thus increasing catalyst stability [74].

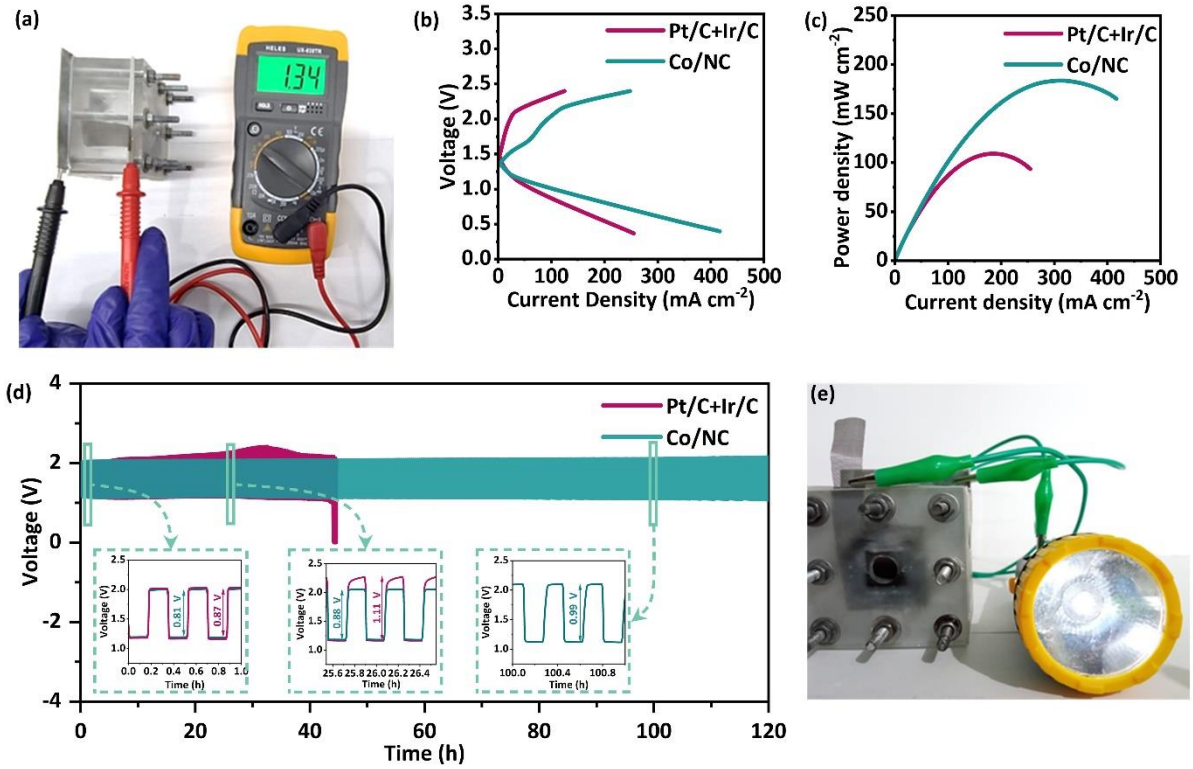

Figure 5 (a) Photograph of OCV measurement of Co/NC-based Zn-air battery. The comparison of Zn-air battery performance for Co/NC-based and Pt/C+Ir/C-based: (b) galvanodynamic discharge-charge plots, (c) corresponding power density plots, and (d) stability cycling curves measured at 10 mA cm^{-2}. (e) Photograph of a flashlight powered by a Co/NC-based Zn-air battery.

With favorable bifunctional OER/ORR performance and stability of Co/NC, we present the construction of rechargeable Zn–air batteries utilizing Co/NC as the air-cathode, polished Zn plate as the anode, and electrolyte of 0.15 M ZnO + 6 M KOH. As shown in Figure 5(a), the Co/NC-based Zn–air battery results in 1.34 V open-circuit voltage (OCV). The battery performance was then investigated by conducting galvanodynamic charge and discharge tests. Co/NC-based battery performs better than the benchmark Pt/C+Ir/C-based battery (Figure 5(b)). Co/NC-based battery shows a narrower voltage gap at 10 mA cm^{-2} (0.18 V) than that for Pt/C+Ir/C (0.39 V), indicating excellent rechargeability [75]. This lower voltage gap highlights the advantage of the Co/NC with foam-like structures and homogeneous Co nanoparticles, assuring efficient charge transfer and diffusion of the reactant [76, 77]. Furthermore, From Figure 5(c), Co/NC-based battery can deliver a high power density of 184 mW cm^{-2}, which far exceeds the performance of Pt/C+Ir/C-based battery (109 mW cm^{-2}) and some reported Co-based Zn-air batteries (106-179 mW cm^{-2}) [66, 69, 78, 79], proving the preferable performance of our prepared Co/NC materials.

A charge-discharge stability test was carried out to evaluate the stability of both Co/NC and Pt/C+Ir/C-based Zn-air batteries. The test involved applying a current density of 10 mA cm^{-2} (Figure 5(d)). At the starting time, the voltage difference between the Co/NC and Pt/C+Ir/C-based batteries is around 0.81 V and 0.87 V, respectively (inset figure in Figure 5(d)). Following 25 h stability test, there is a noticeable shift in the voltage gap for Pt/C+Ir/C-based battery to 1.11 V, while Co/NC-based battery only shows a small increase to 0.88 V. This condition relatively remains stable for 120 h stability test, confirming high long-term stability of Co/NC-based battery. The high long-term performance was achieved by a thin carbon layer that encapsulates the Co nanoparticle (Figure 2(d)). This carbon protective layer effectively shielded the internal Co nanoparticles from direct contact with the harsh alkaline electrolyte, preventing the formation of Co^{2+} ions and subsequent oxidation to Co_3O_4 [80, 81]. In this case, carbon encapsulation maintained the stable phase crystallinity of Co after cycling tests, thereby enhancing the overall stability of the zinc-air battery [82-84]. Exploring the related state-of-the-art Co/NC-based Zn–air battery exhibits a satisfactory performance in terms of lifespan, surpassing previously reported values battery life cycle in the range of 40-180 h [65, 69, 79, 85]. In addition, a Zn–air battery with Co/NC can power a flashlight, showcasing its potential in practical applications (Figure 5(e)).

DOI: 10.5614/j.eng.technol.sci.2024.56.5.10

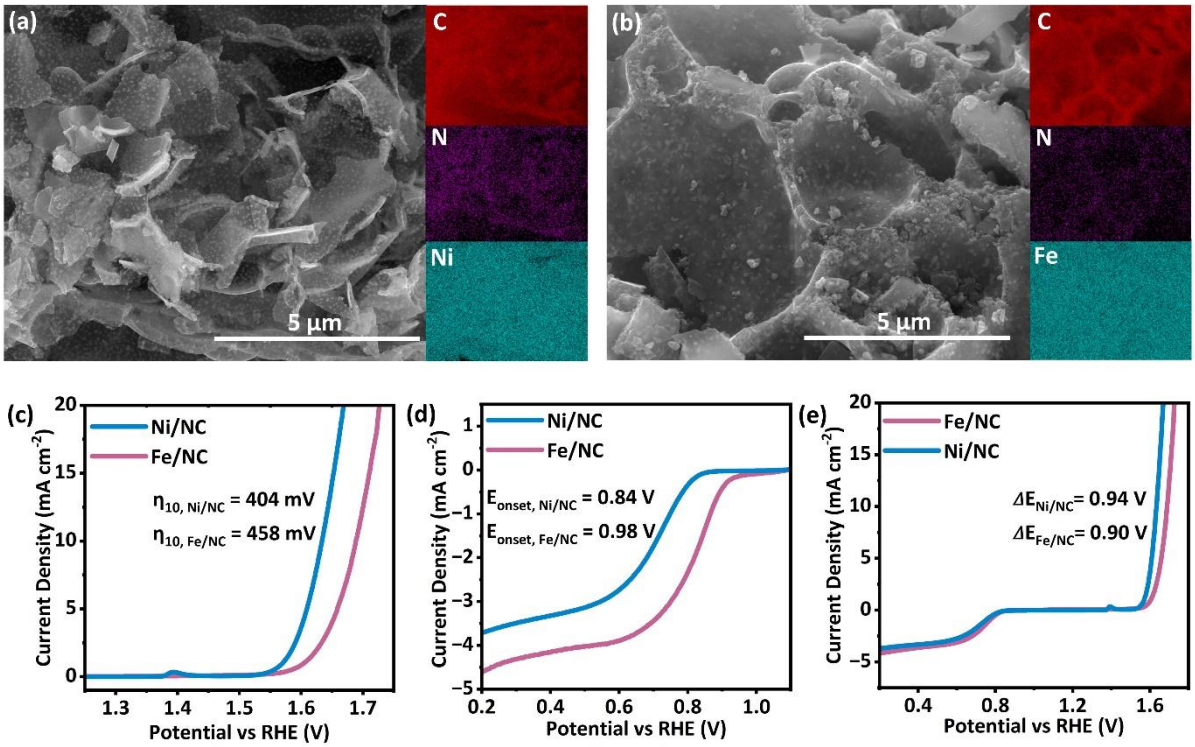

Figure 6 (a) SEM images and EDS mapping for C (red), N (purple), and Ni (cyan) elements. (b) SEM images and EDS mapping for C (red), N (purple), and Fe (cyan) elements. (c) OER polarization curve, (d) ORR polarization curve, and (e) the overall polarization curves for bifunctional catalytic activity of Ni/NC and Fe/NC.

Motivated by the efficiency and straightforwardness of the current solvent-free approach, we expand upon it to synthesize other M/NC catalysts. We can produce Ni/NC and Fe/NC catalysts by replacing the Co nitrate with Ni or Fe nitrate as the metal precursor. Like the Co/NC sample, featured foam-like structures with homogeneous Ni or Fe nanoparticles distribution are also observed in both catalysts (see Figure 6(a) and 6(b)). Ni/NC and Fe/NC also show a good bifunctional OER/ORR performance in alkaline electrolytes (Figure 6(c) and 6(d)), resulting in favorable ΔE values (Figure 6(e)). The results suggest that the developed solvent-free method technique is adaptable in synthesizing various bifunctional M/NC-based catalysts featuring foam-like structures with a homogenous distribution of metal nanoparticles, providing enhanced accessibility for reactants and electrons throughout the reaction.

Conclusion

An eco-friendly and time-effective solvent-free method has been successfully developed to synthesize foam-like structure of Co/NC catalyst. The obtained Co/NC catalyst shows homogeneous Co nanoparticles anchored on porous-rich nitrogen-doped carbon foam, enabling abundant accessible active sites and fast reactant distribution. In addition, Co nanoparticles encapsulated with nitrogen-doped carbon layers may minimize metal dissolution by preventing direct contact between the metal nanoparticles and the electrolyte, thereby increasing catalyst stability. With these excellences, the Co/NC catalyst exhibits high bifunctional OER/OER performances with ΔE of 0.78 and good catalytic stability. In line, Co/NC-based rechargeable Zn-air battery has the ability to deliver a large power density of 184 mW cm^{-2} and is stable for up to 120 h. The developed solvent-free method can also be applied to synthesize Ni/NC and Fe/NC with a foam-like structure, offering possibilities for the versatile fabrication of bifunctional catalysts to promote the advancement of rechargeable Zn-air batteries.

Acknowledgement

We acknowledge financial support from Research, Community Service, and Innovation Program (P2MI) Institut Teknologi Bandung 2024.

Compliance with ethics guidelines

The authors declare that they have no conflict of interest or financial conflicts to disclose.

This article does not contain any studies with human or animal subjects performed by any of the authors.

References

[1] Shao, W., Yan, R., Zhou, M., Ma, L., Roth, C., Ma, T., Cao, S., Cheng, C., Yin, B. & Li, S., *Carbon-Based Electrodes for Advanced Zinc-Air Batteries: Oxygen-Catalytic Site Regulation and Nanostructure Design*, Electrochem. Energy Rev., **6**(1), 11, 2023.

[2] Bi, X., Jiang, Y., Chen, R., Du, Y., Zheng, Y., Yang, R., Wang, R., Wang, J., Wang, X. & Chen, Z., *Rechargeable Zinc–Air versus Lithium–Air Battery: from Fundamental Promises Toward Technological Potentials*, Adv. Energy Mater., **14**(6), 2302388, 2024.

[3] Tian, Y., Xu, L., Li, M., Yuan, D., Liu, X., Qian, J., Dou, Y., Qiu, J. & Zhang, S., *Interface Engineering of CoS/CoO@N-Doped Graphene Nanocomposite for High-Performance Rechargeable Zn–Air Batteries*, Nanomicro Lett., **13**(1), 3, 2020.

[4] Yang, X., Lin, L., Guo, X. & Zhang, S., *Design of Multifunctional Electrocatalysts for ORR/OER/HER/HOR: Janus Makes Difference*, Small, **20**(40), 2404000, 2024.

[5] Lei, H., Tan, S., Ma, L., Liu, Y., Liang, Y., Javed, M.S., Wang, Z., Zhu, Z. & Mai, W., *Strongly Coupled NiCo2O4 Nanocrystal/MXene Hybrid through In Situ Ni/Co–F Bonds for Efficient Wearable Zn–Air Batteries*, ACS Appl. Mater. Interfaces, **12**(40), pp. 44639-44647, 2020.

[6] Akmalia, R., Balqis, F., Andriani, M. F., Irmawati, Y. & Sumboja, A., *Well-Dispersed NiFe Nanoalloy Embedded on N-Doped Carbon Nanofibers as Free-Standing Air Cathode for All-Solid-State Flexible Zinc-Air Battery*, J. Energy Storage, **72**, 108743, 2023.

[7] Ali, Z., Mehmood, M., Ahmed, J. & Nizam, M.N., *Synthesis of Graphitic Nanofibers and Carbon Nanotubes by Catalytic Chemical Vapor Deposition Method on Nickel Chloride Alcogel for High Oxygen Evolution Reaction Activity in Alkaline Media*, Nano-Struct. Nano-Objects, **24**, 100574, 2020.

[8] Yang, F., Gao, X., Xie, J., Liu, X., Jiang, J. & Lu, X., *Cobalt-Based Electrocatalysts as Air Cathodes in Rechargeable Zn–Air Batteries: Advances and Challenges*, Small Struct., **2**(12), 2100144, 2021.

[9] Chen, D., Pan, L., Pei, P., Song, X., Ren, P. & Zhang, L*., Cobalt-Based Oxygen Electrocatalysts for Zinc-Air Batteries: Recent Progress, Challenges, and Perspectives*, Nano Res., **15**(6), pp. 5038-5063, 2022.

[10] Dong, F., Wu, M., Chen, Z., Liu, X., Zhang, G., Qiao, J. & Sun, S., *Atomically Dispersed Transition Metal-Nitrogen-Carbon Bifunctional Oxygen Electrocatalysts for Zinc-Air Batteries: Recent Advances and Future Perspectives*, Nanomicro Lett., **14**(1), 36, 2021.

[11] Shi, Z., Yang, W., Gu, Y., Liao, T. & Sun, Z., *Metal-Nitrogen-Doped Carbon Materials as Highly Efficient Catalysts: Progress and Rational Design*, Adv. Sci., **7**(15), 2001069, 2020.

[12] Wang, S., Chen, S., Ma, L. & Zapien, J.A., *Recent Progress in Cobalt-Based Carbon Materials as Oxygen Electrocatalysts for Zinc-Air Battery Applications*, Mater. Today Energy, **20**, 100659, 2021.

[13] Fiorio, J.L., Garcia, M.A.S., Gothe, M.L., Galvan, D., Troise, P.C., Conte-Junior, C.A., Vidinha, P., Camargo, P.H.C. & Rossi, L.M., Recent Advances in the Use of Nitrogen-Doped Carbon Materials for the Design of Noble Metal Catalysts, Coord. Chem. Rev., **481**, 215053, 2023.

[14] Liu, Y., Dong, P., Li, M., Wu, H., Zhang, C., Han, L. & Zhang, Y., Cobalt Nanoparticles Encapsulated in Nitrogen-Doped Carbon Nanotube as Bifunctional-Catalyst for Rechargeable Zn-Air Batteries, Front. Mater., **6**, 85, 2019.

[15] Ma, L., Chen, S., Pei, Z., Huang, Y., Liang, G., Mo, F., Yang, Q., Su, J., Gao, Y., Zapien, J.A. & Zhi, C., *Single-Site Active Iron-Based Bifunctional Oxygen Catalyst for a Compressible and Rechargeable Zinc–Air Battery*, ACS Nano, **12**(2), pp. 1949-1958, 2018.

[16] Liu, G., Xia, X., Zhao, C., Zhang, X. & Zhang, W., *Ultrafine Ni Nanoparticles Anchored on Carbon Nanofibers as Highly Efficient Bifunctional Air Electrodes for Flexible Solid-State Zinc-Air Batteries*, J. Colloid Interface Sci., **588**, pp. 627-636, 2021.

[17] Choi, E.Y., Kim, D.E., Lee, S.Y., Park, C.B. & Kim, C.K., *Cobalt Nanoparticles-Encapsulated Holey Nitrogen-Doped Carbon Nanotubes for Stable and Efficient Oxygen Reduction and Evolution Reactions in Rechargeable Zn-Air Batteries*, Appl. Catal. B: Environ., **325**, 122386, 2023.

[18] Ding, J., Wang, P., Ji, S., Wang, H., Linkov, V. & Wang, R., *N-Doped Mesoporous FeNx/Carbon as ORR and OER Bifunctional Electrocatalyst for Rechargeable Zinc-Air Batteries, Electrochim.* Acta, **296**, pp. 653-661, 2019.

DOI: 10.5614/j.eng.technol.sci.2024.56.5.10

[19] Fuku, X., Dyosiba, X. & Iftikhar, F.J., *Green Prepared Nanomaterials from Various Biodegradable Wastes and Their Application in Energy*, Nano-Struct. Nano-Objects, **35**, 100997, 2023.

[20] Zhou, K.-Y., Chen, G.-Y., Liu, J.-A., Zhang, Z.-P., Sun, P., Zhang, W.-Z., Niu, F., Zhang, W.-X. & Liang, J.-C., *Cobalt Nanoparticles Encapsulated in N-Doped Graphene Nanoshells as an Efficient Cathode Electrocatalyst for a Mechanical Rechargeable Zinc–Air Battery*, RSC Adv., **6**(93), pp. 90069-90075, 2016.

[21] Chen, S., Ma, L., Wu, S., Wang, S., Li, Z., Emmanuel, A. A., Huqe, M. R., Zhi, C. & Zapien, J. A., *Uniform Virus-Like Co–N–Cs Electrocatalyst Derived from Prussian Blue Analog for Stretchable Fiber-Shaped Zn–Air Batteries*, Adv. Funct. Mater., **30**(10), 1908945, 2020.

[22] Wang, Z., Xiao, S., Zhu, Z., Long, X., Zheng, X., Lu, X. & Yang, S., *Cobalt-Embedded Nitrogen Doped Carbon Nanotubes: A Bifunctional Catalyst for Oxygen Electrode Reactions in a Wide pH Range*, ACS Appl. Mater. Interfaces, **7**(7), pp. 4048-4055, 2015.

[23] Zhang, W., Yao, X., Zhou, S., Li, X., Li, L., Yu, Z. & Gu, L., *ZIF-8/ZIF-67-Derived Co-Nx-Embedded 1D Porous Carbon Nanofibers with Graphitic Carbon-Encased Co Nanoparticles as an Efficient Bifunctional Electrocatalyst*, Small, 14(24), pp. 1800423, 2018.

[24] Li, Y., Jia, B., Fan, Y., Zhu, K., Li, G. & Su, C.-Y., *Bimetallic Zeolitic Imidazolite Framework Derived Carbon Nanotubes Embedded with Co Nanoparticles for Efficient Bifunctional Oxygen Electrocatalyst*, Adv. Energy Mater., **8**(9), pp. 1702048, 2018.

[25] Wang, Z., Zhang, H., Zhang, X., Wang, X. & Zhang, X., *Solvent-Free and Large-Scale Synthesis of SiOx/C Nanocomposite with Carbon Encapsulation for High-Performance Lithium-Ion Battery Anodes*, Compos. B. Eng., **247**, 110308, 2022.

[26] Wang, Z., Hou, X., Dekyvere, S., Mousavi, B. & Chaemchuen, S., *Single-Thermal Synthesis of Bimetallic Co/Zn@NC under Solvent-Free Conditions as an Efficient Dual-Functional Oxygen Electrocatalyst in Zn–Air Batteries*, Nanoscale, **14**(44), pp. 16683-16694, 2022.

[27] Irmawati, Y., Tan, D.A., Balqis, F., Iskandar, F. & Sumboja, A., *Trifunctional Electrocatalysts Based on a Bimetallic Nanoalloy and Nitrogen-Doped Carbon with Brush-Like Heterostructure*, Nanoscale, **16**(4), pp. 1833-1842, 2024.

[28] Wang, J., Liu, M., Chaemchuen, S., Klomkliang, N., Kao, C.-M. & Verpoort, F., *Carbon-Supported Cobalt Nanoparticles via Thermal Sugar Decomposition as Efficient Electrocatalysts for the Oxygen Evolution Reaction*, ACS Appl. Nano Mater., **5**(6), pp. 7993-8004, 2022.

[29] Han, H., Chao, S., Bai, Z., Wang, X., Yang, X., Qiao, J., Chen, Z. & Yang, L., *Metal-Organic-Framework-Derived Co Nanoparticles Deposited on N-Doped Bimodal Mesoporous Carbon Nanorods as Efficient Bifunctional Catalysts for Rechargeable Zinc−Air Batteries*, ChemElectroChem, **5**(14), pp. 1868-1873, 2018.

[30] Irmawati, Y., Balqis, F., Destyorini, F., Adios, C.G., Yudianti, R., Iskandar, F. & Sumboja, A., *Cobalt Nanoparticles Encapsulated with N-Doped Bamboo-Like Carbon Nanofibers as Bifunctional Catalysts for Oxygen Reduction/Evolution Reactions in a Wide pH Range*, ACS Appl. Nano Mater., **6**(4), pp. 2708-2718, 2023.

[31] Liu, J., Ma, J., Tang, K., Wang, R., Wu, Y., Qu, C. & Wu, M., *MOF-Derived Nanocarbon Materials Loaded with Bimetallic Sulfides as Cathode Catalysts for Zinc–Air Batteries*, New J Chem, **47**(20), pp. 9870-9878, 2023.

[32] Zhao, Y., Li, M., Shi, Q., Li, B., Hu, Z., Li, J., Wan, X. & Yu, H., *Co/C Composites Generated from Biomass Exhibit Outstanding Electromagnetic Wave Absorption*, Diam. Relat. Mater, **138**, 110191, 2023.

[33] Chen, M., Han, S., Sun, M., Huang, J., Li, Z., Xu, Y., Cheng, G. & Yu, L., *Cobalt Oxide Nanosheets Anchored on Loofah Sponge-Derived Carbon as a High-Performance Bifunctional Electrocatalyst for Rechargeable Zinc-Air Batteries*, J. Alloys Compd., **971**, 172511, 2023.

[34] Luo, L., Xu, Y., Wang, D. & Qiu, X., *Dispersed Cobalt Nanoparticles in the Nitrogen Doped Carbon Black as Efficient Catalysts for Oxygen Reduction Reaction and Zinc-Air Batteries*, Chem. Eng. Sci., **273**, 118654, 2023.

[35] Zhang, X., Luo, J., Lin, H.-F., Tang, P., Morante, J. R., Arbiol, J., Wan, K., Mao, B.-W., Liu, L.-M. & Fransaer, J., *Tailor-Made Metal-Nitrogen-Carbon Bifunctional Electrocatalysts for Rechargeable Zn-Air Batteries via Controllable MOF Units*, Energy Storage Mater., **17**, pp. 46-61, 2019.

[36] Deng, S.-Q., Zhuang, Z., Zhou, C.-A., Zheng, H., Zheng, S.-R., Yan, W. & Zhang, J., *Metal-Organic Framework Derived FeNi Alloy Nanoparticles Embedded In N-Doped Porous Carbon as High-Performance Bifunctional Air-Cathode Catalysts for Rechargeable Zinc-Air Battery*, J. Colloid Interface Sci., **641**, pp. 265-276, 2023.

[37] Li, Y., Liu, Q., Zhang, S. & Li, G., *The Vital Balance of Graphitization and Defect Engineering for Efficient Bifunctional Oxygen Electrocatalyst Based on N-doping Carbon/CNT Frameworks*, ChemCatChem, **11**(2), pp. 861-867, 2019.

[38] Cai, J.-J., Zhou, Q.-Y., Liu, B., Gong, X.-F., Zhang, Y.-L., Goh, K., Gu, D.-M., Zhao, L., Sui, X.-L. & Wang, Z.-B., *Sponge-Templated Sandwich-Like Cobalt-Embedded Nitrogen-Doped Carbon Polyhedron/Graphene Composite as a Highly Efficient Catalyst for Zn–Air Batteries*, Nanoscale, **12**(2), pp. 973-982, 2020.

[39] Irmawati, Y., Balqis, F., Persada, P.B., Destyorini, F., Yudianti, R., Iskandar, F. & Sumboja, A., *Iron-Decorated Nitrogen/Boron co-Doped Reduced Graphene Oxide Aerogel for Neutral Rechargeable Zn-Air Batteries*, Batteries, **9**(7), 356, 2023.

[40] Liu, Y., Wu, X., Guo, X., Lee, K., Sun, Q., Li, X., Zhang, C., Wang, Z., Hu, J., Zhu, Y., Leung, M.K.H. & Zhu, Z., *Modulated FeCo Nanoparticle in Situ Growth on the Carbon Matrix for High-Performance Oxygen Catalysts*, Mater. Today Energy, **19**, 100610, 2021.

[41] Irmawati, Y., Prakoso, B., Balqis, F., Indriyati, Yudianti, R., Iskandar, F. & Sumboja, A., *Advances and Perspective of Noble-Metal-Free Nitrogen-Doped Carbon for pH-Universal Oxygen Reduction Reaction Catalysts*, Energy Fuels, **37**(7), pp. 4858-4877, 2023.

[42] Chen, M., Wu, Y., Zhou, Y., Yu, X., Dai, P., Yu, J., Jiang, T. & Wu, M., *A Leaf-Like Porous N-Doped Carbon Structure Embedded with CoS2 Nanoparticles Self-Supported on Carbon Fiber Paper as a Cathode in Flexible Zinc–Air Batteries*, New J Chem, **47**(19), pp. 9297-9306, 2023.

[43] Faisal, S.N., Haque, E., Noorbehesht, N., Zhang, W., Harris, A.T., Church, Tamara L. & Minett, A.I., *Pyridinic and Graphitic Nitrogen-Rich Graphene for High-Performance Supercapacitors and Metal-Free Bifunctional Electrocatalysts for ORR And OER*, RSC Adv., **7**(29), pp. 17950-17958, 2017.

[44] Wang, Y., Pan, Y., Zhu, L., Yu, H., Duan, B., Wang, R., Zhang, Z. & Qiu, S., *Solvent-Free Assembly of Co/Fe-Containing MOFs Derived N-Doped Mesoporous Carbon Nanosheets for ORR And HER*,, Carbon, **146**, pp. 671-679, 2019.

[45] Zhang, W., Pei, S., Xu, K., Han, Z., Ma, J., Zhang, Y., Liu, G. & Xu, X., *Co,N-Doped Carbon Sheets Prepared by a Facile Method as High-Efficiency Oxygen Reduction Catalysts*, RSC Adv., **12**(52), pp. 33981-33987, 2022.

[46] Yang, Y., Bu, Y., Long, X.-l., Zhou, Z.-k., Wang, J. & Cai, J.-j., *Synthesis of Co—N—C Catalysts from a Glucose Hydrochar and Their Efficient Hydrogenation of Nitrobenzene*, New Carbon Mater., **38**(3), pp. 555-563, 2023.

[47] Huang, G., Wang, Y., Zhang, T., Wu, X. & Cai, J., *High-Performance Hierarchical N-Doped Porous Carbons from Hydrothermally Carbonized Bamboo Shoot Shells for Symmetric Supercapacitors*, J. Taiwan Inst. Chem. Eng., **96**, pp. 672-680, 2019.

[48] Kim, M., Kim, H.S., Yoo, S.J., Yoo, W.C. & Sung, Y.-E., *The Role of Pre-Defined Microporosity in Catalytic Site Formation for the Oxygen Reduction Reaction in Iron- and Nitrogen-Doped Carbon Materials*, J. Mater. Chem. A, 5(8), pp. 4199-4206, 2017.

[49] Liang, H.-W., Wei, W., Wu, Z.-S., Feng, X. & Müllen, K., *Mesoporous Metal–Nitrogen-Doped Carbon Electrocatalysts for Highly Efficient Oxygen Reduction Reaction*, J. Am. Chem. Soc., **135**(43), pp. 16002-16005, 2013.

[50] Notodarmojo, S., Sugiyana, D., Handajani, M., Kardena, E. & Larasati, A., *Synthesis of TiO2 Nanofiber-Nanoparticle Composite Catalyst and Its Photocatalytic Decolorization Performance of Reactive Black 5 Dye from Aqueous Solution*, J. Eng. Technol. Sci., **49**(3), pp. 340-356, 2017.

[51] Sun, T., Wang, J., Qiu, C., Ling, X., Tian, B., Chen, W. & Su, C., *B, N Codoped and Defect-Rich Nanocarbon Material as a Metal-Free Bifunctional Electrocatalyst for Oxygen Reduction and Evolution Reactions*, Adv. Sci., **5**(7), pp. 1800036, 2018.

[52] Huang, R., Wen, Y., Peng, H. & Zhang, B., *Improved Kinetics of OER on Ru-Pb Binary Electrocatalyst by Decoupling Proton-Electron Transfer*, Chinese J. Catal., **43**(1), pp. 130-138, 2022.

[53] Balqis, F., Irmawati, Y., Geng, D., Nugroho, F.A.A. & Sumboja, A., *Nanostructured Ball-Milled Ni–Co–Mn Oxides from Spent Li-Ion Batteries as Electrocatalysts for Oxygen Evolution Reaction*, ACS Appl. Nano Mater., **7**(16), pp. 18138-18145, 2024.

[54] Farid, S., Ren, S., Tian, D., Qiu, W., Zhao, J., Zhao, L., Mao, Q. & Hao, C., *3D Flower-Like Polypyrrole-Derived N-Doped Porous Carbon Coupled Cobalt Oxide as Efficient Oxygen Evolution Electrocatalyst*, Int. J. Hydrogen Energy., 45(56), pp. 31926-31941, 2020.

[55] Yuan, W., Wang, S., Ma, Y., Qiu, Y., An, Y. & Cheng, L., *Interfacial Engineering of Cobalt Nitrides and Mesoporous Nitrogen-Doped Carbon: Toward Efficient Overall Water-Splitting Activity with Enhanced Charge-Transfer Efficiency*, ACS Energy Lett., **5**(3), pp. 692-700, 2020.

[56] Makertihartha, I., Subagjo, S. & Gunawan, M.L., *Synthesis and Activity Test of Cu/ZnO/Al2O3 for the Methanol Steam Reforming as a Fuel Cellâs Hydrogen Supplier*, J. Eng. Technol. Sci., **41**(1), pp. 37-49, 2013.

[57] Liu, J., Dang, J., Wang, M., Wang, X., Duan, X., Yuan, S., Liu, T. & Wang, Q., *Metal–Organic-Framework-Derived Cobalt Nanoparticles Encapsulated in Nitrogen-Doped Carbon Nanotubes on Ni Foam Integrated Electrode: Highly Electroactive and Durable Catalysts for Overall Water Splitting*, J. Colloid Interface Sci., **606**, pp. 38-46, 2022.

[58] Zhang, J., Zhang, T., Ma, J., Wang, Z., Liu, J. & Gong, X., *ORR and OER of Co–N Codoped Carbon-Based Electrocatalysts Enhanced by Boundary Layer Oxygen Molecules Transfer*, Carbon, **172**, pp. 556-568, 2021.

[59] Zhang, Y., Zhang, G., Zhang, M., Zhu, X., Shi, P., Wang, S. & Wang, A.-L., *Synergistic Electronic and Morphological Modulation by Trace Ir Introduction Boosting Oxygen Evolution Performance over a Wide pH Range*, Chem. Eng. J., **433**, 133577, 2022.

DOI: 10.5614/j.eng.technol.sci.2024.56.5.10

[60] Fan, L., Du, X., Zhang, Y., Li, M., Wen, M., Ge, X., Kang, Z. & Sun, D., *N,P-Doped Carbon with Encapsulated Co Nanoparticles as Efficient Electrocatalysts for Oxygen Reduction Reactions*, Dalton Trans., **48**(7), pp. 2352-2358, 2019.

[61] Wei, C., Wang, H., Eid, K., Kim, J., Kim, J.H., Alothman, Z.A., Yamauchi, Y. & Wang, L., *A Three-Dimensionally Structured Electrocatalyst: Cobalt-Embedded Nitrogen-Doped Carbon Nanotubes/Nitrogen-Doped Reduced Graphene Oxide Hybrid for Efficient Oxygen Reduction*, Chem. Eur. J., **23**(3), pp. 637-643, 2017.

[62] Lu, Q., Yu, J., Zou, X., Liao, K., Tan, P., Zhou, W., Ni, M. & Shao, Z., *Self-Catalyzed Growth of Co, N-Codoped CNTs on Carbon-Encased CoSx Surface: A Noble-Metal-Free Bifunctional Oxygen Electrocatalyst for Flexible Solid Zn–Air Batteries*, Adv. Funct. Mater., **29**(38), 1904481, 2019.

[63] Yang, L., Shi, L., Wang, D., Lv, Y. & Cao, D., *Single-Atom Cobalt Electrocatalysts for Foldable Solid-State Zn-Air Battery*, Nano Energy, **50**, pp. 691-698, 2018.

[64] Wu, Y., Nagata, S. & Nabae, Y., *Genuine Four-Electron Oxygen Reduction over Precious-Metal-Free Catalyst in Alkaline Media*, Electrochim. Acta, **319**, pp. 382-389, 2019.

[65] Zhou, B., Liu, Y., Wu, X., Liu, H., Liu, T., Wang, Y., Mehdi, S., Jiang, J. & Li, B., *Wood-Derived Integrated Air Electrode with Co-N Sites for Rechargeable Zinc-Air Batteries*, Nano Res., **15**(2), pp. 1415-1423, 2022.

[66] Peng, X., Wei, L., Liu, Y., Cen, T., Ye, Z., Zhu, Z., Ni, Z. & Yuan, D., *Cobalt Nanoparticles Embedded in N-Doped Carbon Nanotubes on Reduced Graphene Oxide as Efficient Oxygen Catalysts for Zn-Air Batteries*, Energy Fuels, **34**(7), pp. 8931-8938, 2020.

[67] Meng, L., Liu, W., Lu, Y., Liang, Z., He, T., Li, J., Nan, H., Luo, S. & Yu, J., *Lamellar-Stacked Cobalt-Based Nanopiles Integrated with Nitrogen/Sulfur Co-Doped Graphene as a Bifunctional Electrocatalyst for Ultralong-Term Zinc-Air Batteries*, J. Energy Chem., **81**, pp. 633-641, 2023.

[68] Tan, M., Xiao, Y., Xi, W., Lin, X., Gao, B., Chen, Y., Zheng, Y. & Lin, B., *Cobalt-Nanoparticle Impregnated Nitrogen-Doped Porous Carbon Derived from Schiff-Base Polymer as Excellent Bifunctional Oxygen Electrocatalysts for Rechargeable Zinc-Air Batteries*, J. Power Sources, **490**, 229570, 2021.

[69] Gao, B., Tan, M., Xi, W., Lin, X., Li, Z., Shen, M. & Lin, B., *Co-Embedded Carbon Nanotubes Modified N-Doped Carbon Derived from Poly(Schiff Base) and Zeolitic Imidazole Frameworks as Efficient Oxygen Electrocatalyst Towards Rechargeable Zn-Air Battery*, J. Power Sources, **527**, 231205, 2022.

[70] Gebreslase, G. A., Sebastián, D., Martínez-Huerta, M.V., Tsoncheva, T., Tsyntsarski, B., Georgiev, G. & Lázaro, M.J., *CoFe-loaded P, N Co-Doped Carbon Foam Derived from Petroleum Pitch Waste: An Efficient Electrocatalyst for Oxygen Evolution Reaction*, Catal. Today, **423**, 113991, 2023.

[71] Qian, C., Guo, X., Zhang, W., Yang, H., Qian, Y., Xu, F., Qian, S., Lin, S. & Fan, T., *Co_3O_4 Nanoparticles on Porous Bio-Carbon Substrate as Catalyst for Oxygen Reduction Reaction*, Microporous Mesoporous Mater., **277**, pp. 45-51, 2019.

[72] Li, L., Chen, J., Wang, S., Huang, Y. & Cao, D., MOF-Derived Con/Cofe/NC Bifunctional Electrocatalysts for Zinc-Air Batteries, Appl. Surf. Sci., **582**, 152375, 2022.

[73] Mashola, T.A., Matthews, T., Msomi, P.F. & Maxakato, N.W., *Novel Nanostructured Electrocatalysts for Fuel Cell Technology: Design, Solution Chemistry-Based Preparation Approaches and Application*, Nano-Struct. Nano-Objects, **29**, 100831, 2022.

[74] Qian, G., Chen, J., Luo, L., Zhang, H., Chen, W., Gao, Z., Yin, S. & Tsiakaras, P*., Novel Bifunctional V2O3 Nanosheets Coupled with N-Doped-Carbon Encapsulated Ni Heterostructure for Enhanced Electrocatalytic Oxidation of Urea-Rich Wastewater*, ACS Appl. Mater. Interfaces, **12**(34), pp. 38061-38069, 2020.

[75] Mahbub, M.A.A., Adios, C. G., Xu, M., Prakoso, B., LeBeau, J.M. & Sumboja, A., *Red Bean Pod Derived Heterostructure Carbon Decorated with Hollow Mixed Transition Metals as a Bifunctional Catalyst in Zn-Air Batteries*, Chem. Asian J., **16**(17), pp. 2559-2567, 2021.

[76] Fu, J., Hassan, F.M., Zhong, C., Lu, J., Liu, H., Yu, A. & Chen, Z., *Defect Engineering of Chalcogen-Tailored Oxygen Electrocatalysts for Rechargeable Quasi-Solid-State Zinc–Air Batterie*s, Adv. Mater., **29**(35), 1702526, 2017.

[77] Dyartanti, E. R., Paramitha, T., Jumari, A., Purwanto, A., Nur, A., Budiman, A. W. & Nisa, S. S., *A Comparative Study of Solid-State and Co-precipitation Methods for Synthesis of NMC622 Cathode Material from Spent Nickel Catalyst*, J. Eng. Technol. Sci., **55**(5), pp. 548-557, 2023.

[78] Liu, J., Xu, L., Deng, Y., Zhu, X., Deng, J., Lian, J., Wu, J., Qian, J., Xu, H., Yuan, S., Li, H. & Ajayan, Pulickel M., *Metallic Cobalt Nanoparticles Embedded in Sulfur and Nitrogen Co-Doped Rambutan-Like Nanocarbons for the Oxygen Reduction Reaction under Both Acidic and Alkaline Conditions*, J. Mater. Chem. A, **7**(23), pp. 14291-14301, 2019.

[79] Jiao, J., Pan, Y., Wang, B., Yang, W., Liu, S. & Zhang, C., *Melamine-Assisted Pyrolytic Synthesis of Bifunctional Cobalt-based Core–Chell Electrocatalysts for Rechargeable Zinc–Air Batteries*, J. Energy Chem., **53**, pp. 364-371, 2021.

[80] Mehboob, A., Gilani, S. R., Anwar, A., Sadiqa, A., Akbar, S. & Patujo, J., *Nanoscale Cobalt-Oxide Electrocatalyst for Efficient Oxygen Evolution Reactions in Alkaline Electrolyte*, J. Appl. Electrochem., **51**(4), pp. 691-702, 2021.

[81] Babu, C.R., Avani, A.V., Shaji, S. & Anila, E.I., *Electrochemical Characteristics of Co_3O_4 Nanoparticles Synthesized via the Hydrothermal Approach for Supercapacitor Applications*, J. Solid State Electrochem., **28**(7), pp. 2203-2210, 2024.

[82] Liu, X., Huo, S., Xu, X., Wang, X., Zhang, W., Chen, Y., Wang, C., JiahaoXie, Liu, X., Chang, H. & Zou, J., *Carbon Nanotube-Encapsulated Co/Co3Fe7 Heterojunctions as a Highly-Efficient Bifunctional Electrocatalyst for Rechargeable Zinc-Air Batteries*, J. Colloid Interface Sci., **666**, pp. 296-306, 2024.

[83] Chen, X., Pu, J., Hu, X., Yao, Y., Dou, Y., Jiang, J. & Zhang, W., *Janus Hollow Nanofiber with Bifunctional Oxygen Electrocatalyst for Rechargeable Zn–Air Battery*, Small, **18**(16), 2200578, 2022.

[84] Singhal, R. & Kalra, V., *Cobalt Nanoparticle-Embedded Porous Carbon Nanofibers with Inherent N- and F-Doping as Binder-Free Bifunctional Catalysts for Oxygen Reduction and Evolution Reactions*, ChemPhysChem, **18**(2), pp. 223-229, 2017.

[85] Yan, Q., Sun, R.-M., Wang, L.-P., Feng, J.-J., Zhang, L. & Wang, A.-J., *Cobalt Nanoparticles/ Nitrogen, Sulfur-Codoped Ultrathin Carbon Nanotubes Derived from Metal Organic Frameworks as High-Efficiency Electrocatalyst for Robust Rechargeable Zinc-Air Battery*, J. Colloid Interface Sci., **603**, pp. 559-571, 2021.

Manuscript Received: 17 June 2024
Revised Manuscript Received: 8 August 2024
Accepted Manuscript: 29 August 2024